BMB
Reports

Rationalization of allosteric pathway in *Thermus* sp. GH5 methylglyoxal synthase

Shekufeh Zareian[1], *Khosro Khajeh*[1,*], *Mohammad Pazhang*[2] *& Bijan Ranjbar*[3]

[1]Department of Biochemistry, Faculty of Biological Sciences, Tarbiat Modares University, Tehran, [2]Department of Cellular and Molecular Biology, Faculty of Science, Azarbaijan University of Tarbiat Moallem, Tabriz, [3]Department of Biophysics, Faculty of Biological Sciences, Tarbiat Modares University, Tehran, Iran

A sequence of 10 amino acids at the C-terminus region of methylglyoxal synthase from *Escherichia coli* (EMGS) provides an arginine, which plays a crucial role in forming a salt bridge with a proximal aspartate residue in the neighboring subunit, consequently transferring the allosteric signal between subunits. In order to verify the role of arginine, the gene encoding MGS from a thermophile species, *Thermus* sp. GH5 (TMGS) lacking this arginine was cloned with an additional 30 bp sequence at the 3´-end and then expressed in form of a fusion TMGS with a 10 residual segment at the C-terminus (TMGS$^+$). The resulting recombinant enzyme showed a significant increase in cooperativity towards phosphate, reflected by a change in the Hill coefficient (*n*H) from 1.5 to 1.99. Experiments including site directed mutagenesis for Asp-10 in TMGS and TMGS$^+$, two dimentional structural survey, fluorescence and irreversible thermoinactivation were carried out to confirm this pathway. [BMB Reports 2012; 45(12): 748-753]

INTRODUCTION

Allostery is the regulation of the protein function and structure and/or flexibility induced by the binding of a ligand or another protein (effector) to a site which is generally far from the active site of the protein. Therefore, allostery is the coupling of conformational changes between two separated sites. By this description, allostery is an intrinsic property of all proteins. Effectors that elevate the protein functions including ligand affinity or catalytic rate are named allosteric activators, while those that lower the function are known as allosteric inhibitors. Previously, allostery and cooperativity were limited to multimeric proteins but today it has also been recognized as a property of monomeric proteins (1).

Methylglyoxal synthase (MGS) (EC 4.2.3.3) catalyzes an elimination reaction that converts dihydroxyacetone phosphate (DHAP) to phosphate and pyruvaldehyde, which subsequently tautomerizes to form methylglyoxal (MG) (2, 3), in the first step of the methylglyoxal bypass of the glycolysis pathway (4-6). In the absence or presence of phosphate, MGS kinetic data are hyperbolic or sigmoidal depending on the substrate concentration, respectively (7, 8). Therefore, phosphate acts as an allosteric inhibitor (conformational) and not a product inhibitor (7). The MGS enzyme has been studied in many different organisms (9-13). However, *Escherichia coli* (*E. coli*) MGS is the most extensively studied enzyme (6, 8, 14-16).

Given the importance of product of this enzyme for scientific applications, it has been well explored; however, biological function of this substance in the metabolic pathway is still not very well known. MG is tightly bound to glycolysis from an evolutionary perspective. Although it is not in the main stream of glycolytic pathway but a role can be assigned to its production in phosphate deficiency conditions, as phosphate is one of product of the related reaction (4, 17). It has been suggested that this enzyme in *E. coli* and other microorganisms may facilitate the transition between starvation and abundance (18). MG is converted either to D-lactate via the glyoxalase system or to 1,2-propandiol (a commercial commodity with industrial significance) by glycerol dehydrogenase and aldehyde reductase (4, 19, 20).

Previous studies have revealed different pathways for transition of allosteric signals from ligand to substrate binding and active sites. According to the crystallographic structure of *E. coli* MGS and mutagenic studies, two mechanisms have been proposed for transition of allosteric signals between subunits. According to the first mechanism, formation of a salt bridge between Asp-20 and Arg-150 in the presence of phosphate passes information between the six adjacent subunits. In the second putative mechanism, Pro-92, Arg-107, and Val-111 are employed in this convey (16).

Here, we have studied MGS from a thermophile species, *Thermus* sp. GH5 (TMGS) and its allosteric regulation has been compared with *E. coli* MGS (EMGS). In the previous report (21), we analyzed the oligomerization of TMGS by size

*Corresponding author. Tel & Fax: 021-82884717; E-mail: khajeh@modares.ac.ir
http://dx.doi.org/10.5483/BMBRep.2012.45.12.11-138

Received 1 August 2011, Revised 11 August 2011, Accepted 19 December 2011

Keyword: Allosteric pathway, Cooperativity, Hill coefficient, Methylglyoxal synthase, Structural compactness

ISSN: 1976-6696 (print edition) / 1976-670X (electronic edition)

exclusion chromatography, which showed the active fraction was related to the hexameric state (21). On the other hand, the crystallographic state of this enzyme shows the hexameric form (PDBID: 2X8W). In addition, TMGS has Hill coefficient (*n*H) of 1.5 in the presence of phosphate (21). Since TMGS has a lower *n*H compared to EMGS (7, 8), we focused on their structures at the C-terminus and assumed that the absence of the essential arginine at this terminal and consequently lack of salt bridge can be the main reason for the lower response to the transition of allosteric effects. Therefore, a segment contains 10 residues was added to TMGS C-terminus and its impact on salt bridge formation and *n*H was investigated. In order to confirm the role of the arginine in salt bridge formation, two additional variants, with alteration at an aspartate residue were designed. Structural features of these protein variants were also studied using circular dichroism (CD) and fluorescence spectroscopy.

RESULTS

Addition of C-terminal tail to TMGS elevated the Hill coefficient

Multiple amino acid sequence alignment of TMGS (132 residues) and *E. coli* MGS, a well-studied MGS with 152 residues, revealed that these two enzymes can show significant structural differences due to the loss of 20 residues in TMGS, especially the 10 amino acids that are essential for the configuration of the C-terminus α-helix in *E. coli* MGS (Supplementary data, Fig. S1). Saadat and Harrison have previously introduced two allosteric signal transition pathways in the *E. coli* enzyme, one of which happens through introduction of a salt bridge between Asp-20 and Arg-150 (16). This pathway is missing in the TMGS variant due to the loss of 10 amino acids as well as the lack of the necessary arginine at the C-terminus end. On the other hand, the comparison between the *n*H of TMGS (1.5) (21) and EMGS (3.4) shows a clear difference in the ability of these two enzymes in transition of the allosteric signals. However, many reasons can cause such difference, such as complete or partial cooperativity that is propounded in allosteric enzymes. It is assumed that the lack of a salt bridge in TMGS could be one of the reasons for lower allosteric response. Therefore, the question is whether the addition of an extra peptide to the C-terminus can raise the sensitivity of the enzyme to phosphate by engaging the proximal aspartate in the salt bridge.

Therefore, by designing a 60-nucleotide reverse primer, a ten amino acid sequence (YQRYLADRLK), was appended to the C-terminus of TMGS, and the addition was confirmed by gene sequencing. The new enzyme with 142 amino acid residues was called TMGS$^+$. Moreover, the effect of this segment and subsequent changes of the *n*H should be validated.

Cloning of the enzyme coding sequence was performed in the pET-21a vector and the fusion protein was expressed in the BL21 strain of *E. coli*. The Enzyme was further purified by heat shock and anion exchange chromatography (data not shown). Furthermore, SDS-PAGE analysis revealed the distinction between the mass of TMGS (14.3 kDa) and TMGS$^+$ (15.6 kDa) as predicted (Supplementary data, Fig. S2).

Kinetic parameters of TMGS$^+$ and TMGS were calculated from the direct assay of MGS, described in the methods section, using DHAP as a substrate and inorganic phosphate as an allosteric inhibitor. *n*H was raised from 1.5 in TMGS to 1.99 in TMGS$^+$ which revealed the effect of arginine at position 140. Mutations were designed in both TMGS$^+$ and TMGS to assess the salt bridge arrangement between Arg-140 and the proximal aspartate at position 10 in TMGS$^+$ (equal to Asp-20 in EMGS).

Mutation of Asp-10 to Asn confirmed the salt bridge arrangement in TMGS$^+$

TMGSD10N and TMGS$^+$D10N mutants were constructed, using the quick change method. Cloning, expression and purification of enzymes were done as described above. The kinetic parameters and Hill coefficients were also calculated. Comparison of these parameters in four variants could reveal the effect of the embedded Arg-140 and subsequent formation of a salt bridge between this arginine and Asp-10.

In spite of an increase in TMGS$^+$ *n*H from 1.5 to 1.99, this coefficient did not raise in TMGS$^+$D10N despite the presence of a C-terminal Arg-140. Furthermore, the TMGSD10N variant did not show any sensibility to this mutation. K_m, k_{cat} and catalytic efficiency of the mutants and their *n*H, in 0 and 1.5 mM phosphate are presented in Table 1. In addition, the Michaelis-Menten curve and Hill plot of four variants are depicted in Fig. 1. The formation of the helical structure as a result of tail attachment to TMGS was investigated by secondary structure analysis using circular dichroism spectra measurements.

Circular dichroism spectra of TMGS and TMGS$^+$

The Segment added to the TMGS C-terminus was assumed to form a helical structure like its equivalent part in EMGS. Structural studies were performed to confirm the presence of an α-helical structure as an efficient spatial structure for arrangement of a salt bridge. As seen in Fig. 2 helical structure of the TMGS$^+$ was increased compared to TMGS. Further, the Enzymes compactness and thermal stability were measured by intrinsic fluorescence and irreversible thermoinactivation assay.

Table 1. Kinetic parameters of TMGS, TMGS$^+$ and two mutated enzymes

	K_m (mM)	k_{cat} (s^{-1})	k_{cat}/K_m	*n*H[a]
Thermus sp. GH5				
MGS (TMGS)	0.50 ± 0.02	326.4 ± 2	652.9	1.50
TMGS$^+$	0.21 ± 0.01	102.9 ± 1	490.0	1.99
TMGS D10N	0.75 ± 0.03	0.41 ± 0.02	0.544	1.40
TMGS$^+$ D10N	0.25 ± 0.01	0.09 ± 0.004	0.374	1.44

[a]Hill coefficient is for 1.5 mM concentration of phosphate.

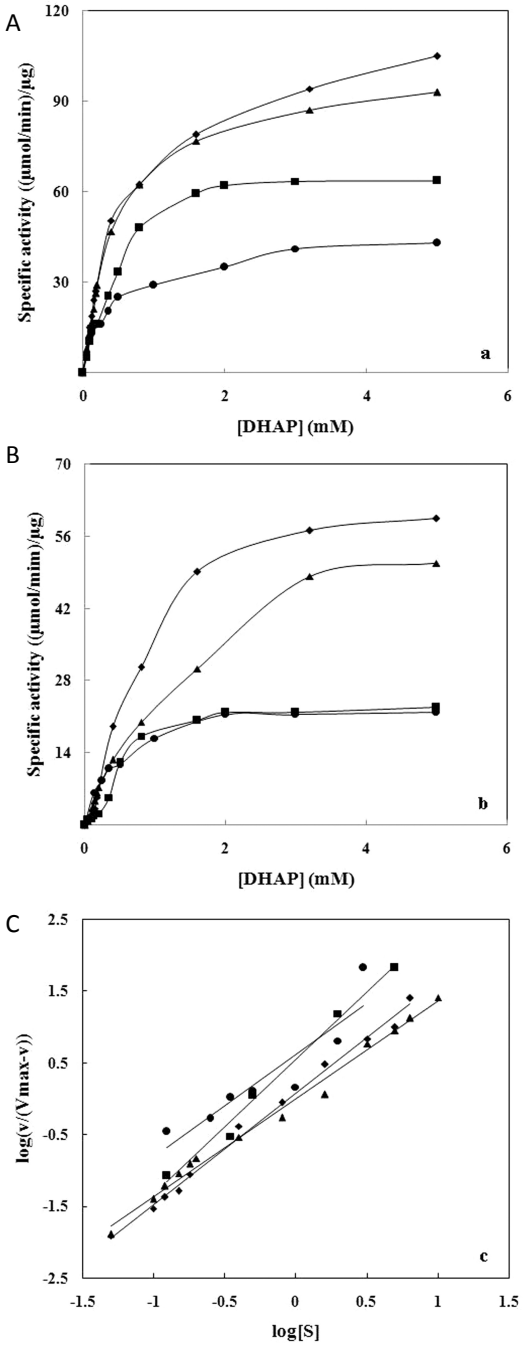

Fig. 1. Michaelis-Menten curve and Hill plot of four variants in different concentrations of DHAP as substrate. (A) 0 mM phosphate, (B) 1.5 mM phosphate (C) Hill plot of four variants. Hill plot was drawn according to the equation mentioned in the Materials and Methods section, in the presence of 1.5 mM of phosphate. (♦) TMGS, (▲) TMGS D10N, (■) $TMGS^+$, (●) $TMGS^+$D10N.

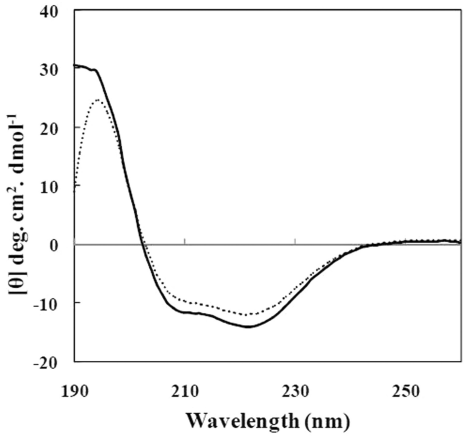

Fig. 2. Far-UV CD spectra of TMGS (----) and $TMGS^+$ (—). Diagram reveals a more helical structure for $TMGS^+$.

Intrinsic fluorescence

It is assumed that $TMGS^+$ has a more compact structure than TMGS due to the formation of a salt bridge in its structure. The fluorescence emission of a protein is the result of its intrinsic fluorophores such as tryptophan and tyrosine residues. The emission spectrum of these aromatic residues is highly sensitive to their surrounding environment. Structural changes in protein may expose the internal tryptophan residues to aqueous environment or burry the accessible residues in the core of the protein. Alterations in the polarity of tryptophan microenvironment will change the emission spectrum, therefore, it is possible to indirectly follow the conformational changes of the enzyme through its intrinsic fluorescence emission. Upon excitation at 280 and 293 nm, TMGS and $TMGS^+$ showed maximum emission intensity at 340 nm but $TMGS^+$ demonstrated a much higher intensity. Since more structural compactness leads to a higher intensity we assume that a salt bridge might have formed between two adjacent subunits (Asp-10 and Arg-140) that may bury some of the fluorophores in a more hydrophobic microenvironment (Fig. 3).

Irreversible thermoinactivation study of TMGS and $TMGS^+$ to compare structural stability

Thermal inactivation of $TMGS^+$ and TMGS was performed in support of the fluorescence spectroscopy data. The results show that $TMGS^+$ with a half life of 10 min was more stable than TMGS with a half life of 3 min, at 80°C, which suggests a more compact and stable structure in $TMGS^+$. The results are depicted in Fig. S3.

DISCUSSION

The aim of this study was to explore a phenomenon observed by our group (21), which revealed that methylglyoxal synthase from *Thermus* sp. GH5 (TMGS) has a lower *n*H (1.5) com-

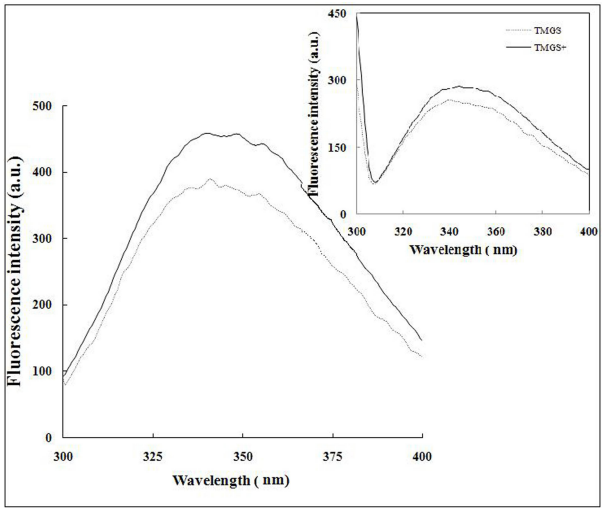

Fig. 3. Fluorescence emission spectra of TMGS (- - - -) and $TMGS^+$ (—) at 280 nm excitation wavelengths, the inset is the spectra for the excitation at 293 nm. Graphs represent more compact structure for $TMGS^+$.

pared to MGS from *Escherichia coli* (EMGS) (3.4). The experiments aimed to identify the reason for lower sensitivity to phosphate concentration and consequently weaker transmission of allosteric signals between neighboring subunits in TMGS. In a study by Saadat and Harrison, two pathways of transmitting the allosteric effect have been proposed for the *E. coli* MGS. In the first possible mechanism, formation of a salt bridge between Asp-20 and Arg-150 was proposed in presence of phosphate that passes on the information between the six adjacent subunits, while in the second proposed mechanism, Pro-92, Arg-107, and Val-111 are employed in this convey. The three amino acids involved in the second pathway are highly conserved among different strains; however, the first pathway has been lost in TMGS due to the absence of the essential arginine which participates in salt bridge formation between subunits. Therefore, to investigate the effect of salt bridge formation on cooperativity we decided to add a segment (10 residues) containing the mentioned arginine to the C-terminus end. An increase in *n*H from 1.5 to 1.99 was observed. Further investigations were required to verify the effect of salt bridge formation on the enzyme cooperativity. For this reason, a mutation (Asp-10 to Asn) was introduced in the protein. Results were in good agreement with the previous data as the *n*H returned to its original value in the $TMGS^+$D10N variant. On the other hand, *n*H of TMGS, did not show any response to the substitution of Asp to Asn, (TMGSD10N mutant). Therefore, the presence of this pathway and conveyance of an allosteric crosstalk through the neighboring subunits to the active site of $TMGS^+$ can be concluded.

The fact that the *n*H in TMGS has not increased as much as it did in EMGS can be explained as follows: First, the possibility of the presence of other pathways for transition of allosteric signals in EMGS. Second, the matter of complete and partial cooperativity could be the reason for high *n*H value obtained in EMGS that may have complete cooperativity and the third reason might be the experimental errors caused by calculation of this coefficient in different time periods.

The possibility that the appended segment adopts an α-helical structure like its equivalent part in EMGS was tested by CD analysis. The CD spectra demonstrated a more helical structure in $TMGS^+$ in comparison with TMGS. However, this data is not an evidence of structural compactness due to formation of salt bridge between Arg-140 and Asp-10 in $TMGS^+$. Fluorescence spectroscopy data demonstrated a more compact structure for $TMGS^+$ compared to TMGS, which could be explained by a salt bridge formation between adjacent subunits. Addition of two tyrosines to $TMGS^+$ tail could be the main cause of higher fluorescence intensity at 340 nm when excited at 280 nm; therefore the samples were also excited at 293 nm, which specially reveals the tryptophan emission in both enzymes. On the other hand, $TMGS^+$ shows a higher thermal stability at 80°C.

Overall, in this work, importance of salt bridge formation between Arg-140 and Asp-10 in the creation of cooperative TMGS has been investigated which shows that this pathway could increase *n*H of TMGS from 1.5 to 1.99 but this value is lower than *n*H of EMGS (3.4). To explain high cooperativity of EMGS further investigations are required.

Finally, these experiments may untie a problem in the big hasp of protein science but still the main question remains; why the mesophilic MGS (EMGS) and thermophilic MGS (TMGS) show different responses to the phosphate concentrations and consequently produce different amounts of methylglyoxal. This ability may have been acquired (through evolution) by *E. coli* in the periods of time.

MATERIALS AND METHODS

Chemicals

T4-DNA ligase and restriction enzymes were purchased from Fermentas (Vilnius, Lithuania). Oligonucleotides were synthesized by MWG Company (Germany). Tryptone and yeast extract were from Liofilchem (Roseto degli Abruzzi, Italy). Dihydroxyacetone phosphate was purchased from Sigma-Aldrich (USA). 2,4-Dinitrophenylhydrazine and other chemicals were obtained from Merck (Darmstadt, Germany).

Construction of $TMGS^+$ plasmid

The $TMGS^+$ gene, (TMGS with additional 30 bp at 3´-end) was constructed using pET-21a plasmid containing the TMGS gene as a template (21). 0.08 μM forward (5´-GGAATTCCATATGCGAGCCCTTGCCCTCATTG-3´) and reverse (5´-CGGAAGCTTCTATTTAAGACGGTCTGCAAGATAACGCTGATATTGGCCCTGGGGGGTTTG-3´) primers were used to amplify $TMGS^+$, in the presence of 1.25 unit taq-polymerase (with an

annealing temperature of 72°C) using polymerase chain reaction thermocycler. The resulting fragment (429 bp) digested with *hindIII* and *NdeI* (the underlined bases) and ligated into the similarly digested pET-21a(+) using T4-DNA ligase. The accuracy of final product was confirmed by DNA sequencing.

Mutagenesis

Site directed mutagenesis was carried out, as described by Fisher and colleagues, using Quick-Change method and chemically synthesized oligonucleotide primers (Bioneer, South Korea) (22). Plasmid pET-21a (+) containing the TMGS gene was used as the template. PCR reaction was carried out in the 50 µl volume containing DNA template (10 ng), 10× PCR buffer, 0.2 mM of each dNTP, 0.8 µM of each primer and PWO polymerase (1.25 units). The mixture was heated at 95°C for five minutes and then subjected to 22 cycles of thermal cycling at 94°C for 1 min, 55°C for 1 min and 68°C for 13 min. PCR product was incubated with DpnI at 37°C for 12 h and then transformed to *E. coli* XL1-blue (23). Five clones were randomly selected for sequencing and confirmation of the mutations.

In order to construct TMGS$^+$D10N gene, TMGSD10N gene was used as template and the other steps were carried out as described previously.

Expression and purification of the enzyme

Constructed expression plasmids were transformed into the *E. coli* strain BL21 (DE3), to produce the 15.6 kDa methylglyoxal synthase and its variants. The bacteria containing recombinant plasmids were grown in Luria-Bertani (LB) medium supplemented with ampicillin (100 µg/ml) at 37°C, 220 rpm. IPTG (1 mM) was added to the culture medium once the culture reached an optical density of 0.5 to 0.7 at 600 nm. Subsequently, temperature was lowered from 37 to 30°C suitable for production of adequate amount of protein. After 19 h, cells were harvested by centrifugation at 5,000 rpm for 20 min and resuspended in lysis buffer containing 2 mM imidazole, 1 M NaCl and 50 mM Tris (pH 7.0). The suspension was subjected to sonic disruption and total lysate was centrifuged for 20 min at 12,000 rpm at 4°C. The supernatant underwent heat-shock at 70°C for 15 min, and the precipitated proteins were removed by centrifugation at 14,000 rpm for 20 min at 4°C (freezing followed by heating the supernatant improved the purification efficiency). The resulted supernatant was sufficient for kinetic studies but further purification was performed on Q-Sepharose by FPLC (Amersham Pharmacia, Sweden) for structural studies. Therefore, the supernatant was dialyzed against 20 mM Tris buffer, pH 8.0 and applied onto Q-Sepharose equilibrated with the same buffer. Proteins were eluted with a linear gradient of NaCl (0-1 M) prepared in 20 mM Tris buffer (pH 8.0). The flow rate was set at 3 ml/min, and fractions containing MGS activity were collected. Purity analysis was then performed on SDS-PAGE 12.5% by the method of Laemmli (24). Protein concentration was measured by Bradford method (25), using bovine serum albumin as standard.

Methylglyoxal synthase activity assay

The spectrophotometric assay of Hopper and Cooper (17) was used to determine the enzyme activity. Briefly, 125 µl of 50 mM imidazole buffer (pH 6.0), 10 µl DHAP (15.625 mM) and 10 µl of the enzyme were incubated at 60°C for 5 min. Then 0.1 ml of the mixture was added to 0.33 ml of 2,4-dinitro-phenyhydrazine reagent (0.1% 2,4-dinitro-phenyhydrazine in 2 mM HCl) and followed by mixing with 0.9 ml of distilled water. After incubation in 30°C for 15 min, 1.67 ml NaOH (10% w/v) was added and the appeared purple color was measured at 550 nm after a further 15 minutes incubation. A molar extinction coefficient of 4.48×10^4 was used to calculate the methyglyoxal concentration (7, 14, 26).

Enzyme kinetics

Kinetic parameters were determined as explained above. Mixtures containing different concentrations of DHAP with no enzyme were used as controls and each data point (initial velocity) was determined in triplicate. Steady-state kinetic parameters in the presence and absence of phosphate were fitted to Michaelis-Menten equation and were numerically analyzed by Lineweaver-Burk equation. nH was calculated from the fallowing equation:

$$\log[v / (V_{max} - v)] = n\mathrm{H}\log[\mathrm{S}] - \log(\mathrm{K}')$$

Where v and V_{max} are velocity and maximal velocity of the enzyme, respectively, and *n*H is the Hill coefficient. K´ is related to K_m but also contains terms related to the effect of substrate occupancy at one site on the substrate affinity of the other sites. According to this equation, the value of *n*H can be calculated by plotting $\log[v / (V_{max} - v)]$ against log[S].

Fluorescence measurements

Tryptophan fluorescence of TMGS and TMGS$^+$ was measured using a Perkin Elmer luminescence spectrometer LS 55. Samples were excited at 295 nm and the emission was recorded between 300 to 400 nm. All experiments were carried out at room temperature and protein concentrations were 20 µM in 20 mM Tris buffer (pH 8.0).

Irreversible thermoinactivation

Thermal inactivation of TMGS and TMGS$^+$ was investigated in 50 mM imidazole buffer (pH 6.0) at 80°C. Periodically, Samples were removed, cooled on ice and then residual activity was determined as described above. The untreated sample was used as a control (100% activity).

Circular Dichroism measurements

Far-UV spectra (190-260 nm) were recorded on a Jasco spectropolarimeter J-715 (Tokyo, Japan) using 1 mm path length

quartz cell at the protein concentration of 0.2 mg/ml in 20 mM tris buffer (pH 8.0). Results are presented as molar ellipticity [θ] (deg cm^2 $dmol^{-1}$), based on a mean amino acid residue weight of 110 for TMGS and $TMGS^+$. The molar ellipticity [θ] was calculated from the formula $[\theta]_\lambda = (\theta \times 100\ MWR)/(cl)$, where *c* is the protein concentration in mg/ml, *l* the light path length in centimeters, and θ is the measured ellipticity in degrees wavelength λ. The secondary structure parameters were calculated using J700 CD-JASCO software.

Acknowledgements
The authors express their gratitude to the research council of Tarbiat Modares University and Hi Tech Center, Ministry of Mines and Industries for the financial support during the course of this project.

REFERENCES

1. Goodey, N. M. and Benkovic, S. J. (2008) Allosteric regulation and catalysis emerge via a common route. *Nat. Chem. Biol.* **4**, 474-482.
2. Summers, M. C. and Rose, I. A. (1977) Proton transfer reactions of methylglyoxal synthase. *J. Am. Chem. Soc.* **99**, 4475-4478.
3. Yuan, P. M. and Gracy, R. W. (1977) The conversion of dihydroxyacetone phosphate to methylglyoxal and inorganic phosphate by methylglyoxal synthase. *Arch. Biochem. Biophys.* **183**, 1-6.
4. Cooper, R. A. (1984) Metabolism of methylglyoxal in microorganisms. *Annu. Rev. Microbiol.* **38**, 49-68.
5. Cooper, R. A. and Anderson, A. (1970) The formation and catabolism of methylglyoxal during glycolysis in *Escherichia coli*. *FEBS Lett.* **11**, 273-276.
6. Marks, G. T., Susler, M. and Harrison, D. H. (2004) Mutagenic studies on histidine 98 of methylglyoxal synthase: effects on mechanism and conformational change. *Biochemistry* **43**, 3802-3813.
7. Hopper, D. J. and Cooper, R. A. (1972) The purification and properties of *Escherichia coli* methylglyoxal synthase. *Biochem. J.* **128**, 321-329.
8. Saadat, D. and Harrison, D. H. (1998) Identification of catalytic bases in the active site of *Escherichia coli* methylglyoxal synthase: cloning, expression, and functional characterization of conserved aspartic acid residues. *Biochemistry* **37**, 10074-10086.
9. Cooper, R. A. (1974) Methylglyoxal formation during glucose catabolism by Pseudomonas saccharophila. Identification of methylglyoxal synthase. *Eur. J. Biochem.* **44**, 81-86.
10. Huang, K., Rudolph, F. B. and Bennett, G. N. (1999) Characterization of methylglyoxal synthase from Clostridium acetobutylicum ATCC 824 and its use in the formation of 1, 2-propanediol. *Appl. Environ. Microbiol.* **65**, 3244-3247.
11. Murata, K., Fukuda, Y., Watanabe, K., Saikusa, T., Shimosaka, M. and Kimura, A. (1985) Characterization of methylglyoxal synthase in Saccharomyces cerevisiae. *Biochem. Biophys. Res. Commun.* **131**, 190-198.
12. Ray, S. and Ray, M. (1983) Formation of methylglyoxal from aminoacetone by amine oxidase from goat plasma. *J. Biol. Chem.* **258**, 3461-3462.
13. Tsai, P. K. and Gracy, R. W. (1976) Isolation and characterization of crystalline methylglyoxal synthetase from Proteus vulgaris. *J. Biol. Chem.* **251**, 364-367.
14. Cooper, R. A. (1975) Methylglyoxal synthase. *Methods. Enzymol.* **41**, 502-508.
15. Marks, G. T., Harris, T. K., Massiah, M. A., Mildvan, A. S. and Harrison, D. H. (2001) Mechanistic implications of methylglyoxal synthase complexed with phosphoglycolohydroxamic acid as observed by X-ray crystallography and NMR spectroscopy. *Biochemistry* **40**, 6805-6818.
16. Saadat, D. and Harrison, D. H. (1999) The crystal structure of methylglyoxal synthase from *Escherichia coli*. *Structure* **7**, 309-317.
17. Hopper, D. J. and Cooper, R. A. (1971) The regulation of *Escherichia coli* methylglyoxal synthase; a new control site in glycolysis? *FEBS Lett.* **13**, 213-216.
18. Totemeyer, S., Booth, N. A., Nichols, W. W., Dunbar, B. and Booth, I. R. (1998) From famine to feast: the role of methylglyoxal production in *Escherichia coli*. *Mol. Microbiol.* **27**, 553-562.
19. Inoue, Y. and Kimura, A. (1995) Methylglyoxal and regulation of its metabolism in microorganisms. *Adv. Microb. Physiol.* **37**, 177-227.
20. Thornalley, P. J. (1990) The glyoxalase system: new developments towards functional characterization of a metabolic pathway fundamental to biological life. *Biochem. J.* **269**, 1-11.
21. Pazhang, M., Khajeh, K., Asghari, S. M., Falahati, H. and Naderi-Manesh, H. (2010) Cloning, expression, and characterization of a novel methylglyoxal synthase from *Thermus* sp. strain GH5. *Appl. Biochem. Biotechnol.* **162**, 1519-1528.
22. Sambrook, J., Fritsch, E. F. and Maniatis, T. (1989) *Molecular cloning: a laboratory manual 2nd ed.*, Cold Spring Harbor Laboratory, Cold Spring Harbor harbor, Australia.
23. Sambrook, J. and Russell, D. W. (2001) *Molecular cloning: a laboratory manual 3rd ed.*, Cold Spring Harbor Laboratory Press, Cold Spring Harbor, N.Y., USA.
24. Laemmli, U. K. (1970) Cleavage of structural proteins during the assembly of the head of bacteriophage T4. *Nature* **227**, 680-685.
25. Bradford, M. M. (1976) A rapid and sensitive method for the quantitation of microgram quantities of protein utilizing the principle of protein-dye binding. *Anal. Biochem.* **72**, 248-254.
26. Wells, C. F. (1966) The spectra of 2,4-Dinitrophenylhydrazone anions and the determination of carbonyl compounds in dilute aqueous solution. *Tetrahedron* **22**, 9.